Journal of Applied Microbiology

Journal of Applied Microbiology ISSN 1364-5072

ORIGINAL ARTICLE

Sip18 hydrophilin prevents yeast cell death during desiccation stress

B. Rodríguez-Porrata[1], D. Carmona-Gutierrez[2], A. Reisenbichler[2], M. Bauer[2], G. Lopez[1], X. Escoté[1], A. Mas[1], F. Madeo[2] and R. Cordero-Otero[1]

1 Department of Biochemistry and Biotechnology, University Rovira i Virgili, Tarragona, Spain
2 Institute of Molecular Biosciences, University of Graz, Graz, Austria

Keywords
anhydrobiosis, deletion mutant collection, hydrophilin, *Saccharomyces cerevisiae*, stress tolerance.

Correspondence
Ricardo Cordero-Otero, Department of Biochemistry and Biotechnology, University Rovira i Virgili, Marcel.li D. Str., 43007-Taragona, Spain. E-mail: ricardo.cordero@urv.es

2011/0964: received 10 June 2011, revised 14 November 2011 and accepted 7 December 2011

doi:10.1111/j.1365-2672.2011.05219.x

Abstract

Aims: For this study, we performed a genetic screen of *S. cerevisiae*'s deletion library for mutants sensitive to dehydration stress, with which we aimed to discover cell dehydration–tolerant genes.

Methods and Results: We used a yeast gene deletion set (YGDS) of 4850 viable mutant haploid strains to perform a genome-wide screen for the identification of desiccation stress modifiers. *SIP18 is* among the genes identified as essential for cells surviving to drying/rehydration process. Deletion of *SIP18* promotes the accumulation of reactive oxygen species and enhances apoptotic and necrotic cell death in response to dehydration/rehydration process.

Conclusions: SIP18p acts as an inhibitor of apoptosis in yeast under dehydration stress, as suggested by its antioxidative capacity through the ROS accumulation reduction after an H_2O_2 attack.

Significance and Impact of the Study: To our knowledge, this is the first systematic screen for the identification of putative genes essential to overcoming cell dehydration process. A broad range of identified genes could help to understand why some strains of high biotechnological interest cannot cope with the drying and rehydration treatments. Dehydration sensitivity makes these strains not suitable to be commercialized by yeast manufactures.

Introduction

Anhydrobiotic organisms are widespread in the plant kingdom, in fungi such as *Saccharomyces cerevisiae* and in small animals such as rotifers, nematodes and tardigrades. Anhydrobiosis (desiccation tolerance) is considered as a state of suspended metabolism (stasis) induced by the removal of cell water (Crowe *et al.* 1992). To understand the processes behind desiccation stress resistance of anhydrobiotic organisms, we must address controversial issues such as cell age, longevity, the structural and biochemical properties of anhydrous cytoplasm and metabolic stasis (Potts 2001).

The present study describes a genome-wide screen in *S. cerevisiae* to identify the genes that modify cell mortality after dehydration stress (Singh *et al.* 2005). Among the genes characterized as essential for overcoming the cell-drying/rehydration process, six belong to the group of very hydrophilic proteins known as hydrophilins. This group of proteins is defined by common physicochemical characteristics: (i) a Gly content >6%, (ii) the presence of small amino acids such as Ala and Ser and (iii) a high hydrophilicity index of >1·0 (Battaglia *et al.* 2008). Although the functional role of hydrophilins remains speculative, the fact that the transcripts of most genes encoding hydrophilins are induced in response to osmotic stress suggests that they represent an extensive adaptation to water deficit (Posas *et al.* 2000). The genome of *S. cerevisiae* contains 12 genes encoding proteins with the characteristics of hydrophilins. The ectopic expression of some plant hydrophilins (late embryogenesis abundant, LEA proteins) in yeast confers tolerance to water-deficit conditions (Zhang *et al.* 2000). On the other hand, hydrophilins protect the activities of both malate

dehydrogenase and lactate dehydrogenase, which were measured *in vitro* dehydration tests in the presence or absence of hydrophilins from plants, bacteria and yeast. Under similar conditions, trehalose was required in a 10^5-fold molar excess over hydrophilins to confer the same level of protection, suggesting that they provide protection by means of different mechanisms (Reyes *et al.* 2005). A similar study was conducted with two hydrophilins from nematode and wheat, which were found to prevent the enzyme aggregation under desiccation and freezing stress (Goyal *et al.* 2005). Hydrophilins' properties include their roles as antioxidants and as membrane and protein stabilizers during water stress, either by direct interaction or by acting as a molecular shield (Tunnacliffe and Wise 2007).

With recent advances in tissue engineering, cell transplantation and genetic technology, successful long-term storage of living cells is of critical importance. Even common requirements such as the storage of blood cells in blood banks are still a major problem. The complex regulatory network and the often contradictory results obtained with high eukaryotic cells make the application of an easier model system worth striving for. A number of advantages have made yeast cells the model of choice for anhydrobiotic engineering, including the ease of growth and modification, well-characterized cell physiology, genetics and biochemistry. Yeast promises to provide a better understanding of desiccation-tolerant genetics for potential applications in biomedicine, plant biotechnology, and beverage and bio-ethanol technology.

In this study, we performed a genetic screen of *S. cerevisiae*'s deletion library for mutants sensitive to dehydration stress, with which we aimed to discover cell dehydration–tolerant genes. For one of these identified genes, *SIP18*, we have characterized the effects of overexpression in the corresponding deletion strain, which is sensitive to stress imposition. We also show that Sip18p has an antioxidant capacity and is imported into the nucleus as a response to osmotic change during the dehydration process.

Materials and methods

Strains and plasmid construction

Recombinant DNA techniques were performed according to the standard protocols (Sambrook and Russell 2001). Table 1 summarizes the yeast strains and the plasmids used in this study. The single null mutant collection of strains and the reference strain, all in the BY4742 genetic background, were purchased from EUROSCARF (Frankfurt, Germany). The yeast strain expressing the *GFP-SIP18* chromosomal fusion was purchased from Invitrogen. The genes (*SIP18*, *GRX5*, *RPB4*, *RDH54*, *RIF2*, *ORM2 and HSP30*) were obtained by PCR and cloned into yeast expression vector pGREG505Δh digested with *SalI* and transformed into each of the seven yeast deletion strains Δ*sip18*, Δ*grx5*, Δ*rpb4*, Δ*rdh54*, Δ*rif2*, Δ*orm2* and Δ*hsp30* to create *Δsip18*, GAL_p-*SIP18*; *Δgrx5*, GAL_p-*GRX5*; Δ*rpb4*, GAL_p-*RPB4*; Δ*rdh54*, GAL_p-*RDH54*; Δ*rif2*, GAL_p-*RIF2*; Δ*orm2*, GAL_p-*ORM2*; and Δ*hsp30*, GAL_p-*HSP30*, respectively, where the genes are under the control of the *GAL1* promoter. Transformants were selected by plating on synthetic glucose media devoid of leucine. Leu^+ transformants were picked and re-streaked to single colonies, which were confirmed by PCR and testing for the loss of *LEU* marker. The PCR fragments were obtained using BY4742 genomic DNA as a template together with the primer pairs shown in Table S1. The amplification reactions contained single-strength PCR buffer (Roche, Mannheim, Germany), 1·25 mmol l^{-1} dNTPs, 1·0 mmol l^{-1} $MgCl_2$, 0·3 μmol l^{-1} of each primer, 2 ng μl^{-1} template DNA and 3·5 U DNA polymerase (Roche) in a total volume of 100 μl. PCR was carried out in a PCR Express thermal cycler for 15 cycles: denaturation, 2 min at 94°C; primer annealing, 30 s at 55°C; and primer extension, 1 min at 68°C, for all the reactions.

Growth conditions and desiccation–rehydration process

Yeast strains were grown in shake flasks (150 rpm) in SC media containing 0·17% yeast nitrogen base (Difco), 2% glucose, 0·5% $(NH_4)_2SO_4$ and 25 mg l^{-1} uracil and 42 mg l^{-1} lysine and histidine. Growth curves were determined, and 5×10^7 yeast cell suspensions, measured by microscope cell counting from the stationary phase, were desiccated by exposure to dry air at 28°C for ~20 h. In all cases, 5×10^7 cells were rehydrated into 1-ml final volume of pure water at 37°C for 30 min (Rodríguez-Porrata *et al.* 2008).

Determining the yeast viability

After the rehydration process, the viable cell count was calculated by spreading cell dilutions using a Whitley Automatic Spiral Plater (AES Chemunex Bruz, France) on YPD agar medium. The plates were incubated at 28°C for 48 h, and the CFU were quantified using the PROTOCOL SR/HR counting system software ver. 1.27, supplied by Symbiosis (Cambridge, UK).

Statistical analysis

The results were statistically analysed by one-way ANOVA and the Scheffé test from the statistical software package SPSS 15.1 (SPSS Inc., Chicago, IL). Statistical significance was set at $P < 0·05$.

Table 1 Strains and plasmids used in this study

Strains and plasmids	Relevant characteristics	References
E. coli		
DH5α	*endA1 hsdR17 (rk_ mk +) sup E44 thi1E_ recA1 gyr A, rel A1 D (lacZY A-argF) U169 (B80lacZD M15)*	Gibco-BRL
S. cerevisiae		
BY4742	MATα, his3Δ1, leu2Δ0, lys2Δ0, ura3Δ0	Brachmann *et al.* 1998
Δ*sip18*	BY4742, *sip18::kanMX4*	EUROSCARF
Δ*grx5*	BY4742, *grx5::kanMX4*	EUROSCARF
Δ*rpb4*	BY4742, *rpb4::kanMX4*	EUROSCARF
Δ*rdh54*	BY4742, *rdh54::kanMX4*	EUROSCARF
Δ*rif2*	BY4742, *rif2::kanMX4*	EUROSCARF
Δ*orm2*	BY4742, *orm2::kanMX4*	EUROSCARF
Δ*hsp30*	BY4742, *hsp30::kanMX4*	EUROSCARF
BY4742, GAL_p	BY4742 + pGREG505Δh	This work
Δsip18, GAL_p-*SIP18*	Δ*sip18* + pGREG505si	This work
Δgrx5, GAL_p-*GRX5*	Δ*grx5* + pGREG505gr	This work
Δ*rpb4*, GAL_p-*RPB4*	Δ*rpb4* + pGREG505rp	This work
Δ*rdh54*, GAL_p-*RDH54*	Δ*rdh54* + pGREG505rd	This work
Δ*rif2*, GAL_p-*RIF2*	Δ*rif2* + pGREG505ri	This work
Δ*orm2*, GAL_p-*ORM2*	Δ*orm2* + pGREG505or	This work
Δ*hsp30*, GAL_p-*HSP30*	Δ*hsp30* + pGREG505hs	This work
Δ*sip18*, Gal_p	Δ*sip18* + pGREG505Δh	This work
Δsip18, Gal_p-*GFP-SIP18*	Δ*sip18* + pGREG575Δh, $GAL1_p$-*GFP-SIP18-CYC1*$_t$	This work
GFP-SIP18	BY4742, $SIP18_p$-*GFP-SIP18-SIP18*$_t$	Invitrogen
Plasmids		
pGREG505	$GAL1_p$-*SalI-HIS3-SalI-CYC1*$_t$-*KanMX4-LEU2-bla*	Jansen *et al.* 2005
pGREG505Δh	pGREG505, his3Δ0	This work
pGREG575	$GAL1_p$-*GFP-SalI-HIS3-SalI-CYC1*$_t$-*KanMX4-LEU2-bla*	Jansen *et al.* 2005
pGREG575Δh	pGREG575, *his3Δ0*	This work
pGREG505si	$GAL1_p$-*SIP18-CYC1*$_t$-*KanMX4-LEU2-bla*	This work
pGREG505gr	$GAL1_p$-*GRX5-CYC1*$_t$-*KanMX4-LEU2-bla*	This work
pGREG505rp	$GAL1_p$-*RPB4-CYC1*$_t$-*KanMX4-LEU2-bla*	This work
pGREG505rd	$GAL1_p$-*RDH54-CYC1*$_t$-*KanMX4-LEU2-bla*	This work
pGREG505ri	$GAL1_p$-*RIF2-CYC1*$_t$-*KanMX4-LEU2-bla*	This work
pGREG505or	$GAL1_p$-*ORM2-CYC1*$_t$-*KanMX4-LEU2-bla*	This work
pGREG505hs	$GAL1_p$-*HSP30-CYC1*$_t$-*KanMX4-LEU2-bla*	This work

Tests for apoptotic markers

Dihydroethidium (DHE) staining, Annexin V/PI costaining and TUNEL staining were performed as described by Büttner *et al.* 2006. The same samples were analysed by fluorescence microscopy. To determine the frequencies of morphological phenotypes revealed by TUNEL, DHE and Annexin V/PI double staining, at least 10^6 cells from three independent experiments were evaluated using flow cytometry and BD FACSDIVA software (BD Biosciences, San José, CA).

Microscopy

Cultures of strains harbouring pGREG575 plasmid carrying the *GFP*-tagged gene under the control of the *GAL1* promoter were grown to stationary phase in SC medium. The cells were washed with 1 × PBS buffer (pH 7·4) and fixed with 70% ethanol for 10 min at R.T. After a second wash with 1 × PBS, the cells were stained with DAPI for 15 min in the dark at room temperature, followed by a last 1 × PBS wash. Fluorescence was viewed using a Leica fluorescence microscope (DM4000B; Leica Microsystems, Wetzlar, Germany), and a digital camera (DFC300FX; Leica Microsystems, Heerbrugg, Switzerland) and the LEICA IM50 software (Leica Microsystems, Cambridge, UK) were used for image acquisition.

SDS-PAGE and western blot analysis

Proteins were separated on 10% SDS-PAGE and analysed by Western blot according to Current Protocols in Proteins Science (Coligan *et al.* 2000). Mouse anti-GFP-tag (with 1 : 6000 dilute; Roche) and rabbit anti-actin (with 1 : 8000 dilute; Sigma) monoclonal antibodies were used as the primary antibodies, while goat anti-mouse

antibodies (or anti-rabbit) IgG-conjugated with horseradish peroxidase (with 1 : 4000 dilute; Amersham International, Arlington Heights, IL) were used as the secondary antibodies. The membranes were viewed using ECL Advanced Western Blotting Detection kit (Amersham-GE Healthcare, Buckinghamshire, UK), in accordance with manufacturer's instructions. Images were captured using a FlourChem FC2 Imaging System (Cell Biosciences, San Leandro, CA, USA) and were quantified using IMAGEJ ver.1.41 (National Institutes of Health, USA).

Results

Primary screening of deletion mutants to identify strains with lower viability after stress imposition

The different desiccation tolerance capacities of a collection of 4850 viable mutant haploid strains (BY4742) were assessed using a colony-counting assay as described by Rodríguez-Porrata *et al.* (2011). The CFU (colony forming units)/ml mean value for survival after rehydration were calculated after taking into account viability before drying. Before screening the mutant collection, BY4742 cells were resuspended in both 10% trehalose and pure water, thus setting the reference condition for the evaluation of yeast cell viability prior to screening. While the survival rate of BY4742 in deionized water after rehydration was 20%, cells dried in the presence of trehalose showed 45% viability. It is known that trehalose acts as a membrane protector by reducing the membrane-phase transition temperature during the rehydration process (Rodríguez-Porrata *et al.* 2008). Therefore, we ranked the 4850 mutants in ascending order based on their viability rate to then divide them into five arrays: <10%, 10–19%, 20–39%, 40–60% and >60% viability (Fig. 1). This last group collects 12 unrelated deletion mutants. Of the 4850 mutants, 116 (∼2·4%) were identified as having enhanced desiccation sensitivity and are alphabetically listed by ORF in Table 2. Eighty per cent (94/116) of the mutants with <10% viability corresponded to genes for which a function or genetic role has been determined experimentally or can be predicted (Table 2). Thirty per cent (34/116) of these clustered in the functionally related categories of protein synthesis and biogenesis of cellular components, based on the annotations in the functional categories of the Munich Information Centre for Protein Sequences. The remaining genes were dispersed among the numerous and diverse functional categories (Fig. 1). Fourteen per cent (16/116) of the identified genes are annotated as having human orthologues (Table 2), a value that is significantly higher than the percentage of genes in the yeast genome with mammalian orthologues (around 31%, $P < 1 \times 10^{-10}$) (Botstein *et al.* 1997). Among the 23 deletion mutants identified as falling into the functional category of stress response with <10% viability, seven of them normally show gene activation in response to different kinds of stress, including (i) DNA damage response (*RDH54*, Smirnova *et al.* 2004 and *RIF2*, Teixeira *et al.* 2004), (ii) osmotic stress response (*SIP18* Miralles and Serrano 1995), (iii) oxidative stress (*GRX5* Rodríguez-Manzaneque *et al.* 1999) and (iv) general stress response (*RPB4* Miyao *et al.* 2001; *ORM2* Hjelmqvist *et al.* 2002; and *HSP30* Piper *et al.* 1997). We next characterized the effects of increasing Grx5p, Rpb4p, Sip18p, Rdh54p, Rif2p, Orm2p and Hsp30p levels in stationary-state cells, using a plasmid that allows the expression of their encoding genes under the control of the *GAL1* promoter (*pGAL1*) in the corresponding yeast gene deletion strain. Only the transformants overexpressing *GRX5* (GlutaRedoXin), *SIP18* (salt-induced protein) and *RIF2* (Rap1p-interacting factor) displayed at least 40% higher viability than the wild-type strain expressing the empty vector (Fig. 2). No correlation between the kind of stress response genes and viability was observed in these overexpressing strains. Of these three genes, only *SIP18* has shown early transcriptional response during the process of drying and rehydration (Singh *et al.* 2005). Therefore, we prioritized the study of Sip18p to determine whether a correlation exists between intracellular Sip18p abundance and yeast dehydration tolerance.

GFP-SIP18 fusion protein is accumulated in the cytoplasm

With the aim of investigating Sip18p localization, a strain carrying a fusion between Sip18p and green fluorescent protein (GFP) integrated in the *SIP18* locus (*GFP-SIP18*) was microscopically analysed after 24 h in stationary phase, and *SIP18* is mainly expressed during stationary phase (Gasch *et al.* 2000). The fluorescent signal from the GFP-SIP18 fusion protein was minor and uniformly labelled the cells (Fig. 3a), suggesting cytoplasmic localization as has previously been detected (Huh *et al.* 2003). Labelling of the cell surface, nucleus or vacuole system was not observed in any case. To increase the amount of protein within the cell to higher levels than in the wild type, the GFP-Sip18p fusion was placed under the control of the *GAL1* promoter (*GALp*), which is less active than the endogenous *SIP18* promoter in the stationary phase (Gasch *et al.* 2000). The Δ*sip18* strain with the plasmid expressing *GFP-SIP18* under *GALp* after 24-h cultivation in YPD was divided, and cells were observed after 4-h supplementation with 2% galactose or 2% glucose. This fusion was expressed at a very low level in the presence of glucose, resulting in diffuse labelling of the cells mainly because of the low activity of *pGAL* even after glucose

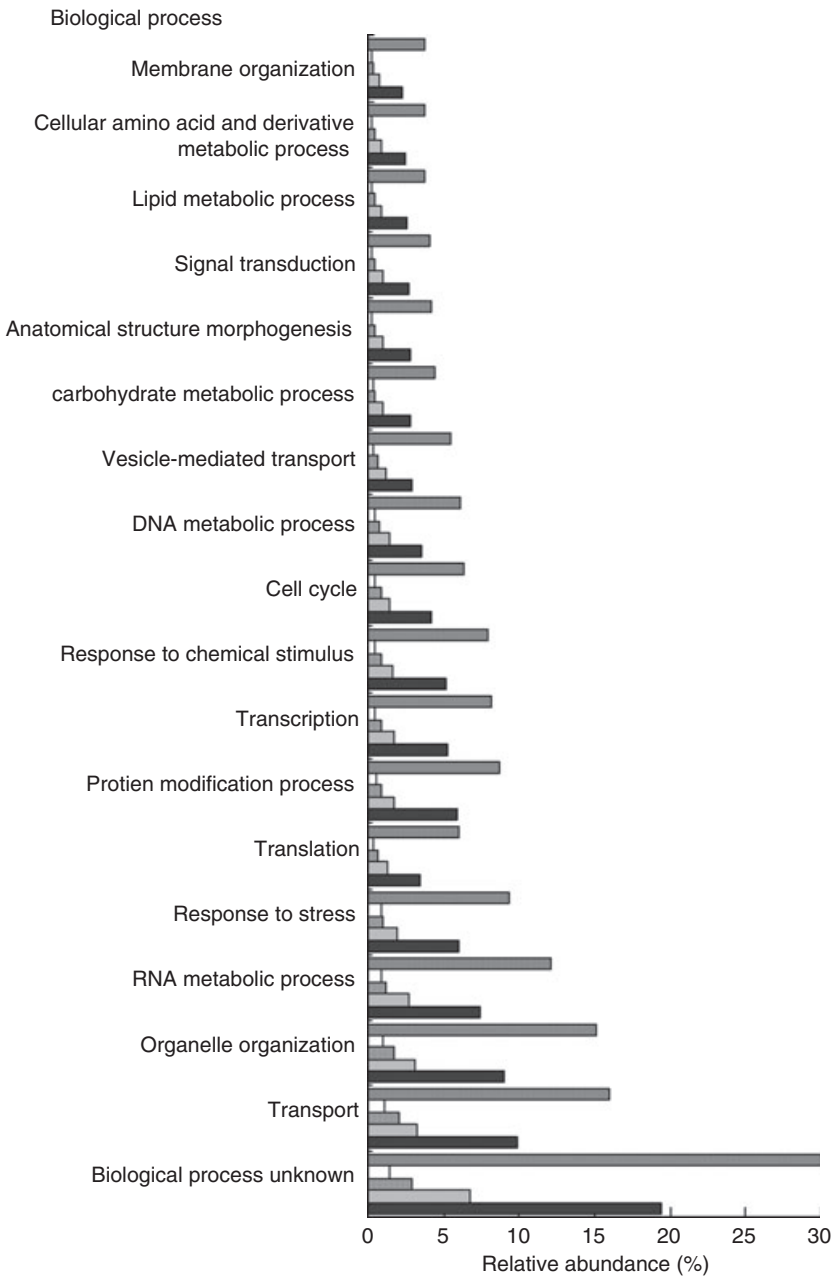

Figure 1 Comparison of the relative percentage of genes in functional categories for the yeast gene deletion set. Around 3% (116/4862) of genes show less of 10% viability after dehydration stress imposition.

starvation. The cytoplasmic localization of GFP-Sip18p in the *GFP-SIP18* cells grown in glucose was similar to the Δ*sip18*, *GAL-GFP-SIP18* cells after glucose supplementation. However, the Δ*sip18*, *GAL-GFP-SIP18* cells supplemented with galactose exhibited a higher fluorescent signal than the cells under the glucose condition and were slightly green-highlighted at the nucleus (Fig. 3a). The *GFP-SIP18* strain expressing the GFP fusion protein did not show significant statistical differences in cell viability when compared with the wild type after stress imposition (Fig. 3b). Additionally, cells from both Δ*sip18*, *GAL-GFP-SIP18* (Fig. 3b) and Δ*sip18*, *GAL-SIP18* strains (Fig. 2) showed the same increase in viability after rehydration. These results allow us to conclude that the addition of the GFP tag did not add/include any phenotypical defect in the viability of the BY4742 strain after the dehydration and rehydration process.

Overexpression of GFP-Sip18p fusion does not result in its import into the nucleus

The cells of the *GFP-SIP18* strain that had undergone 2 days of stationary phase were submitted to different kinds of osmotic stress: 1 mol l^{-1} sorbitol, 1 mol l^{-1}

Table 2 List of mutated strains with less of 10% viability after dehydration stress

Strain	Gene	Function
YBL025W	RRN10	RNA polymerase I-specific transcription initiation factor
YBL033C	RIB1	GTP cyclohydrolase II
YBL038W	MRPL16	Mitochondrial ribosomal protein, large subunit
YBL045C	COR1	Ubiquinol–cytochrome-c reductase 44K core protein
YBL053W		Unknown
YBL057C	PTH2	Aminoacyl-tRNA hydrolase
YBL080C	PET112	Protein required to maintain rho+ mitochondrial DNA
YBR073W	RDH54	Protein required for mitotic diploid-specific recombination and repair and meiosis
YBR146W	MRPS9	Mitochondrial ribosomal protein, small subunit
YBR172C	SMY2	Kinesin-related protein
YBR194W	SOY1	Synthetic with Old Yellow enzyme
YBR267W	REI1	Required for Isotropic bud growth
YBR268W	MRPL37	Mitochondrial ribosomal protein, large subunit
YBR282W	MRPL27	Mitochondrial ribosomal protein, large subunit
YCL003W	PGS1	Phosphatidylglycerophosphate synthase
YCR021C	HSP30	Heat shock protein
YCR045c		Unknown
YCR050c		Unknown
YCR068w	ATG15	Lipase, required for intravacuolar lysis of autophagic bodies
YCR071c	IMG2	Mitochondrial ribosomal protein, large subunit
YCR094w	CDC50	Cell division cycle mutant
YDL020C	RPN4	Transcription factor that stimulates the expression of proteasome genes
YDL039C	PRM7	Pheromone-regulated Membrane protein
YDL044C	MTF2	Mitochondrial protein involved in mRNA splicing and protein synthesis
YDL045W-A	MRP10	Mitochondrial ribosomal protein, small subunit
YDL056W	MBP1	Transcription factor, subunit of the MBF factor
YDL068W		Unknown
YDL091C	UBX3	UBX (ubiquitin regulatory X) domain–containing protein
YDL093W	PMT5	Unknown
YDL107W	MSS2	COX2 pre-mRNA splicing factor
YDL114W		Unknown
YDL133W		Unknown
YDR010C		Unknown
YDR175C	RSM24	Mitochondrial ribosomal protein, small subunit
YDR197W	CBS2	Cytochrome B translational activator protein
YDR204W	COQ4	Responsible for restoring ubiquinone biosynthesis in coq4 mutant
YDR337W	MRPS28	Mitochondrial ribosomal protein, small subunit
YDR350C	TCM10	Protein functions at a post-translational stage in assembly of F0 subunit of mitochondrial ATPase
YDR363W-A	SEM1	Regulator of exocytosis and pseudohyphal differentiation
YDR405W	MRP20	Mitochondrial ribosomal protein, large subunit
YDR432W	NPL3	Nucleolar protein
YDR433W	KRE22	Unknown
YDR511W	ACN9	Protein of gluconeogenesis in mitochondrial intermembrane space
YEL024W	RIP1	Ubiquinol-cytochrome-c reductase iron-sulfur protein precursor
YER087W		Putative prolyl-tRNA synthetase
YER145C	FTR1	High-affinity iron transporter
YER153C	PET122	Translational activator of cytochrome-c oxidase subunit III
YER154W	OXA1	Cytochrome oxidase biogenesis protein
YFL036W	RPO41	DNA-directed RNA polymerase, mitochondrial
YFR032c		Weak similarity to S.pombe polyadenylate-binding protein, YPR112c and Sbp1p
YFR032C-A	RPL29	60S large subunit ribosomal protein
YGR180C	RNR4	Ribonucleotide reductase, small subunit
YGR222W	PET54	Splicing protein and translational activator, mitochondrial
YGR231c	PHB2	Prohibitin
YGR240c	PFK1	6-phosphofructokinase, alpha subunit
YGR243w	FMP43	Unknown

Table 2 (*Continued*)

Strain	Gene	Function
YHL007c	STE20	Cdc42p-activated signal-transducing kinase
YHR011W	DIA4	Probable mitochondrial seryl-tRNA synthetase
YHR038W	RRF1	Mitochondrial ribosome recycling factor
YHR039C-B	VMA10	H^+-transporting ATPase V0 domain 13-KD subunit, vacuolar
YHR079C-B	SAE3	Meiosis-specific protein involved in DMC1-dependent meiotic recombination
YIL084C	SDS3	Transcriptional regulator
YIR021W	MRS1	Protein involved in mitochondrial RNA splicing of COB mRNA
YJL140W	RPB4	DNA-directed RNA polymerase II, 32-kDa subunit
YKR006C	MRPL13	Mitochondrial ribosomal protein, large subunit
YKR009C	FOX2	Hydratase–dehydrogenase–epimerase, peroxisomal
YKR033C		Unknown
YKR085C	MRPL20	Mitochondrial ribosomal protein, large subunit
YKR089C	TGL4	Triacylglycerol lipase involved in TAG mobilization
YKR090W	PXL1	LIM domain-containing protein that localizes to sites of polarized growth, required for selection and/or maintenance of polarized growth sites
YKR098C	UBP11	Ubiquitin C-terminal hydrolase
YLL018C-A	COX19	Protein required for the expression of mitochondrial cytochrome oxidase
YLR136C	TIS11	tRNA-specific adenosine deaminase 3
YLR138W	NHA1	Na+/H+ exchanger (also harbouring K+/H+ activity)
YLR144C	ACF2	Endo-1,3-beta-glucanase
YLR350W	ORM2	Protein required for resistance to agents that induce the unfolded protein response
YLR428C		Unknown
YLR429W	CRN1	A coronin that promotes actin polymerization and cross-linking to microtubules
YLR434C		Protein localized to mitochondria
YLR435W	TSR2	Twenty S rRNA accumulation protein
YLR437C		Conserved hypothetical protein
YLR439W	MRPL4	Mitochondrial ribosomal protein, large subunit
YLR441C	RPS1A	Ribosomal protein S3a.e
YLR453C	RIF2	Rap1p-interacting factor 2
YLR454W	FMP27	Found in Mitochondrial Proteome
YLR456W		Unknown
YMR008C	PLB1	Phospholipase B (lysophospholipase)
YMR009W	ADI1	Aci-reductone dioxygenase involved in the methionine salvage pathway
YMR158C-B		Unknown
YMR158W	MRPS8	Mitochondrial ribosomal protein, small subunit
YMR175W	SIP18	Osmotic stress protein
YMR320W		Hypothetical protein
YNL003C	PET8	Protein of the mitochondrial carrier family (MCF) - unknown function
YNL073W	MSK1	Lysyl-tRNA synthetase, mitochondrial
YNL081C	SWS2	Putative mitochondrial ribosomal protein of the small subunit
YNL248C	RPA49	DNA-directed RNA polymerase A (I) chain, 46 kDa
YNL280C	ERG24	C-14 sterol reductase
YNL294C	RIM21	Regulator of IME2
YNR036C		Unknown
YOR150W	MRPL23	Mitochondrial ribosomal protein, large subunit
YOR155C	ISN1	Inosine 5′-monophosphate (IMP)-specific 5′-nucleotidase catalyses the breakdown of IMP to inosine
YOR158W	PET123	Mitochondrial ribosomal protein, small subunit
YOR305W		Unknown
YOR306C	MCH5	Transporter not monocarboxylate permease
YOR318C		Unknown
YOR333C		Unknown
YOR342C		Unknown
YPL029W	SUV3	ATP-dependent RNA helicase, mitochondrial
YPL059W	GRX5	Glutaredoxin (subfamily Grx3, Grx4 and Grx5)
YPL069C	BTS1	Geranylgeranyl diphosphate synthase
YPL104W	MSD1	Aspartate–tRNA ligase, mitochondrial

Table 2 (*Continued*)

Strain	Gene	Function
YPL183W-A		Unknown
YPR024W	YME1	Protease of the SEC18/CDC48/PAS1 family of ATPases (AAA)
YPR047W	MSF1	Phenylalanine–tRNA ligase alpha chain, mitochondrial
YPR067W	ISA2	Mitochondrial protein required for iron metabolism
YPR099C		Unknown
YPR123C		Unknown

glycerol and 0·75, 0·5 mol l^{-1} NaCl and dehydration. These cells exhibit similar localization in response to dehydration and sorbitol (Fig. 4). However, the cells exposed to NaCl did not reveal any change after up to 3 h of incubation, even when the cells were complemented with 10 or 30 mmol l^{-1} of ascorbic acid (data not shown). To better observe the presence of the full protein in the nuclear compartment, cells of the overexpressing GFP-Sip18p fusion strain were observed after 4 h of galactose induction using a confocal microscope, with a pattern that suggested internal nucleus association (Fig. 4b). Therefore, the nuclear localization of SIP18p in stationary-state cells is mainly driven by osmotic stress. To further increase the amount of protein within the cell, the *pGAL-GFP-SIP18* transformants at the stationary phase were complemented with 2% galactose. Two independent transformants expressing the GFP fusion protein in the stationary phase did not show statistically significant differences in cell viability following stress imposition after 4 h of galactose induction (data not shown). The fluorescent signal from the GFP-Sip18p fusion was monitored during dehydration and rehydration stress. After 4 h of galactose exposure, the cells showed a substantial fluorescent signal from the GFP-Sip18p fusion. The localization of this fluorescence changed from a uniform cell labelling at 0 h to a very slight nuclear localization after 4 h of incubation in the presence of galactose and on to a significant nuclear localization after 4-h drying treatment. At the same time, the strain *GAL-GFP* did not show a clear cellular fluorescent pattern (Fig. 4c). After 30 min of a rehydration process using pure water, we did not see clear cytolocalization of GFP-Sip18p in the cells showing fluorescence. Moreover, even after 1 h of inoculation in YPD media, the fluorescence profile of the rehydrated cells was mainly nuclear (Fig. 4c). These results confirm that the overexpression of the SIP18p fusion did not exhibit any cytolocalization defect in the Δ*sip18*, *pGAL1-GFP-SIP18* strain but did raise the level of the protein enough to produce a remarkable effect on fluorescence and the anti-GFP Western blot detection (Fig. 5b).

Dehydration-tolerant strain shows reduction in apoptotic hallmarks during stress imposition

We wanted to ascertain whether the higher viability rate of Sip18p overexpression compared with that of the wild type after the dehydration and rehydration process could be due to the differences in the apoptotic hallmark

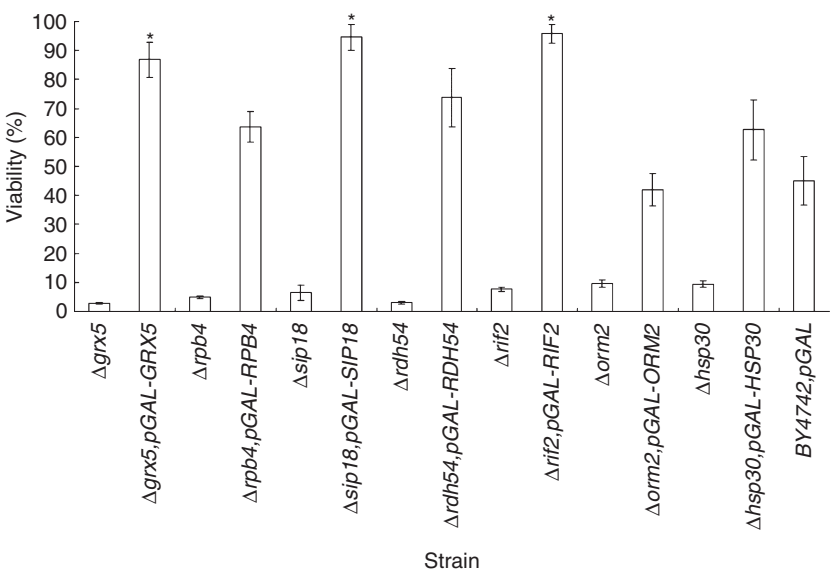

Figure 2 Effect of overexpressing rescue cell genes in yeast viability after cell drying and rehydration. The scale of viability (%) indicates the percentage of experimental values for the different strains. Values shown are means of $n = 3$ independent samples ±SD. *Significant differences ($P \leq 0{\cdot}05$) of the overexpressing strains to *BY4742*, *pGAL* strain.

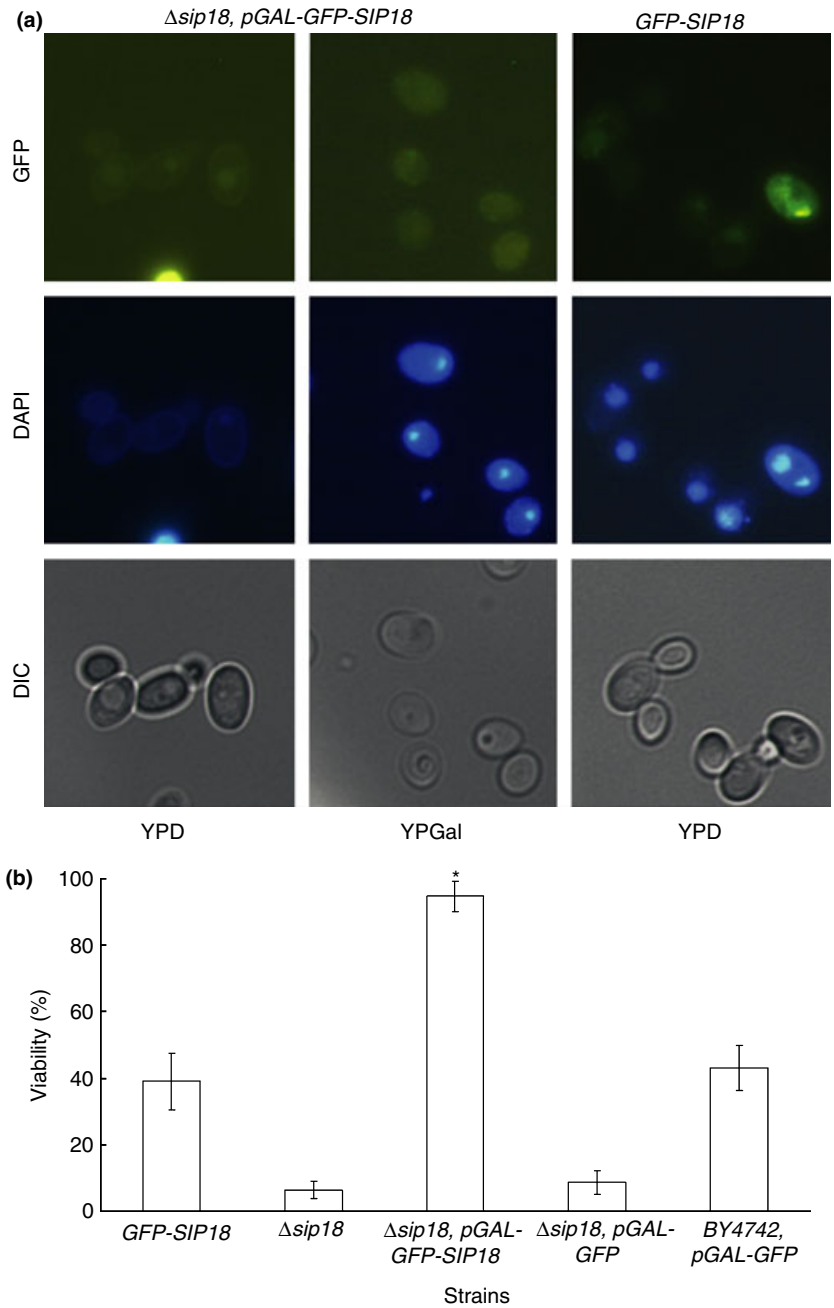

Figure 3 *GFP-SIP18* fusion localized in the cytoplasm. (a) Each column of images shows phase microscopy of the same field, which shows fluorescently labelled green fluorescent protein (GFP), nuclear stained (DAPI) and differential interference contrast (DIC) images of cultured yeast cells. The Δ*sip18* cells transformed with the vector expressing *GFP-SIP18* under *GAL* promoter regulation were photographed after 4 h of galactose (YPGal) or glucose (YPD) supplementation. Cells expressing GFP-SIP18 fusion protein under the *SIP18* promoter were photographed after 24 h in stationary phase. (b) The scale of viability (%) indicates the percentage of experimental values for different strains after stress imposition relative to the highest value for the fresh cultures before cell drying. Values are means of $n = 3$ determinations ±SD. *Significant differences ($P \leq 0{\cdot}05$) compared with *BY4742, pGAL*-GFP strain.

profile. Yeast strains were grown in rich medium, and cells from the stationary phase before desiccation and after rehydration were analysed for apoptotic hallmarks (Madeo *et al.* 1997), such as the accumulation of reactive oxygen species (ROS), phosphatidylserine externalization (Annexin V/PI staining) and DNA-strand breaks (TUNEL assay). Before dehydration, around 20% of Δ*sip18* and Δ*sip18*, *GAL-GFP* cells show fluorescence after DHE incubation, whereas only 15% of Δ*sip18*, *GAL-GFP-SIP18* cells show fluorescence (Fig. 5a). After rehydration, 50% of the reference cells showed intense intracellular DHE staining, but for the overexpressing GFP-Sip18p strain, DHE accumulation only reaches 30%. The next step in our study was to characterize, using flow cytometry, the mode of death accompanying dehydration stress by performing diverse assays using flow cytometry to quantify apoptotic and necrotic markers. Annexin V/propidium iodide (PI) costaining was used to quantify the externalization of phosphatidylserine, an early apoptotic event and membrane permeabilization, which is indicative for necrotic

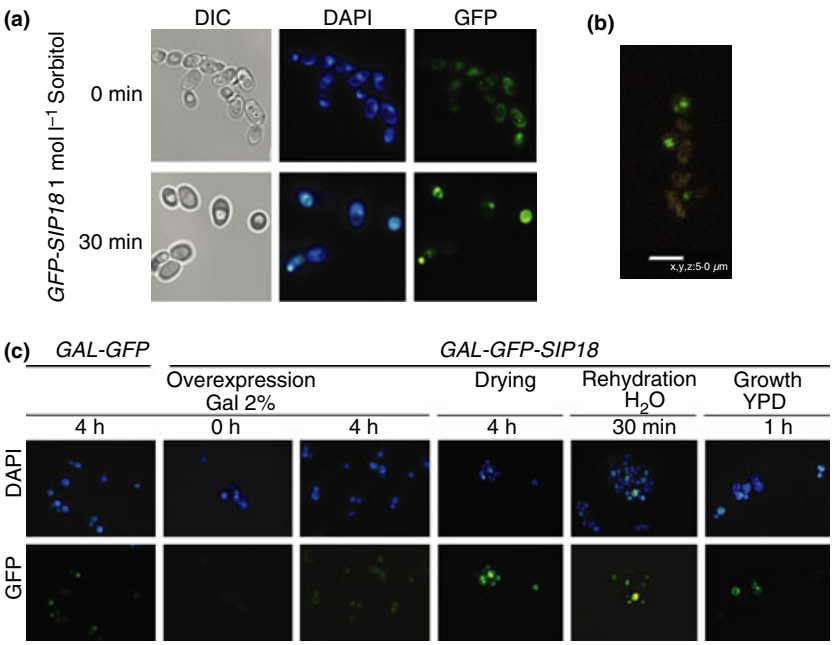

Figure 4 GFP-Sip18p under osmotic stress moves into the nucleus. (a) The cells expressing *GFP-SIP18* under native promoter were photographed before and 30 min after a hyperosmotic shock induced by 1 mol l^{-1} sorbitol, and localization is shown with DAPI fluorescence to visualize the nuclear body. (b) Analysis of hyperosmotic-shocked cells expressing GFP-SIP18p using the confocal microscope. Image generated by the average of a pile of three optical sections. (c) Yeast cells exhibiting SIP18p localization during the dehydration and rehydration process. The *GFP-SIP18* overexpressing cells were photographed at the indicated times of galactose induction, after 4 h of dehydration and 1 h in YPD after a 30-min rehydration treatment. The control overexpressing green fluorescent protein after 4 h of induction does not show a clear localization pattern.

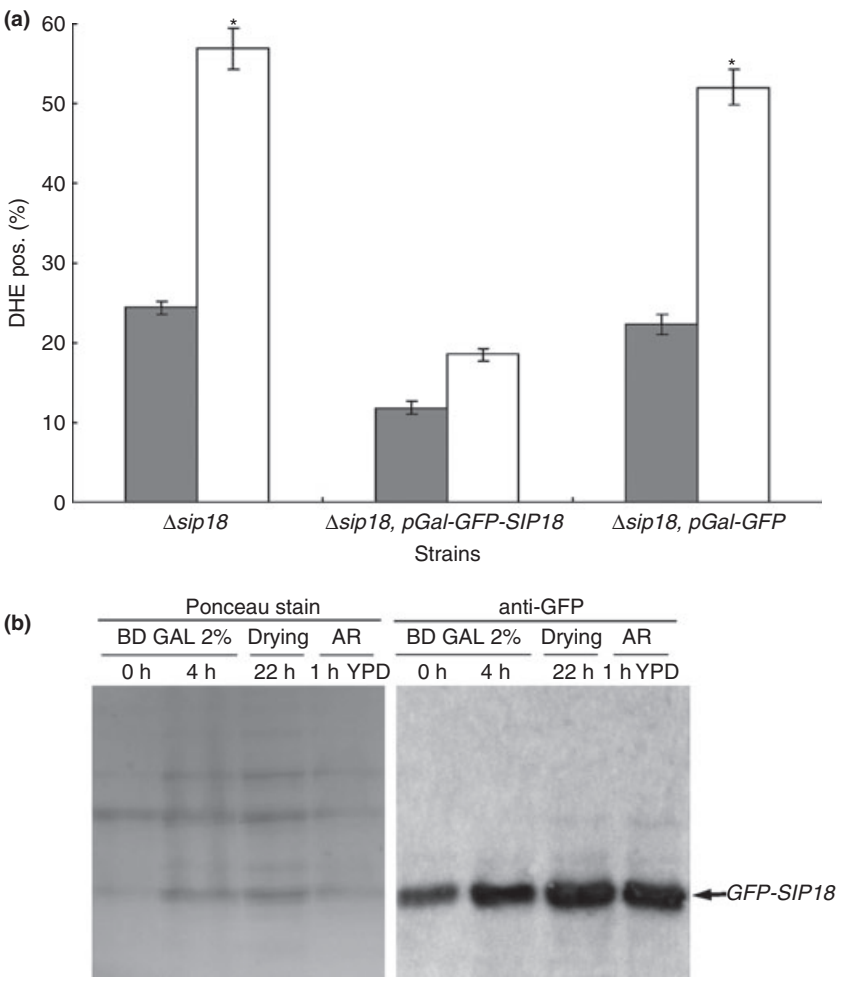

Figure 5 Δ*sip18* cells undergo reactive oxygen species (ROS) accumulation during stress imposition. (a) Quantification of ROS accumulation using DHE staining before drying (grey bars) and after rehydration (white bars). Values are means of $n = 3$ determinations ±SD. DHE pos., DHE-positive cells. *Significant differences ($P \leq 0{\cdot}05$) to before dehydration step. (b) Ponceau stain and Western blot showing GFP-SIP18 protein. Crude extracts from the *GFP-SIP18*-overexpressing cells obtained at the indicated times of galactose induction, after 22-h drying and after 1 h in YPD after a 30-min rehydration treatment were blotted and probed with monoclonal anti-GFP.

death. This staining allows a distinction to be made between early apoptotic (Annexin V positive/PI negative), late apoptotic (Annexin V positive/PI positive) and necrotic (Annexin V negative/PI positive) death. Before dehydration, around 15% of Δ*sip18* and Δ*sip18*, *GAL-GFP* cells are Annexin V^-/PI^+, whereas only 5% of Δ*sip18*, *GAL-GFP-SIP18* cells show necrotic fluorescent profiles at this time. Additionally, the reference and *SIP18*-overexpressing strains have similar values of Annexin V^+/PI^- and Annexin V^+/PI^+ cells, approx. 12 and 5%, respectively (Fig. 6a). After rehydration, the Annexin V^+/PI^- and Annexin V^-/PI^+ cells for all the strains did not exhibit significant statistical differences, approx. 12 and 11%, respectively. Nevertheless, cells from the reference strains showed twice the amounts of Annexin V^+/PI^+ cells as did the overexpressing *GFP-SIP18*. Taking into collective consideration the cell viability results of overexpressing SIP18p strains (Fig. 3b) and the ROS accumulation values (Fig. 5a), we can suggest that there is a correlation between the increase in desiccation survival rate and intracellular ROS levels, imparting a reduction of Annexin V^+/PI^+ cells after stress imposition (Fig. 6).

Dehydration-tolerant strain shows reduction in DHE cells after oxidative stress by H_2O_2

When 4-h galactose-induced cells from the Δ*sip18*; Δ*sip18, GAL-GFP*; and Δ*sip18*, *GAL-GFP-SIP18* strains were subjected to 4 mmol l^{-1} H_2O_2, the overexpressing SIP18p strain showed 50% of reduction in the number of DHE cells after 10 min (Fig. 7). However, at 20 and 40 min, the number of DHE-positive cells was equally affected by H_2O_2 stress, suggesting that SIP18p did not show a strong positive effect on the clearing of H_2O_2. Therefore, we hypothesize that SIP18p plays a physiological role as an antioxidant agent. However, cell mortality after dehydration was present in stationary BY4742 cells supplemented before stress imposition with antioxidant compounds such as ascorbic acid (5, 10 and 30 mmol l^{-1}) and sulfur dioxide (0·15, 0·3 and 0·75 mmol l^{-1}) (data not shown).

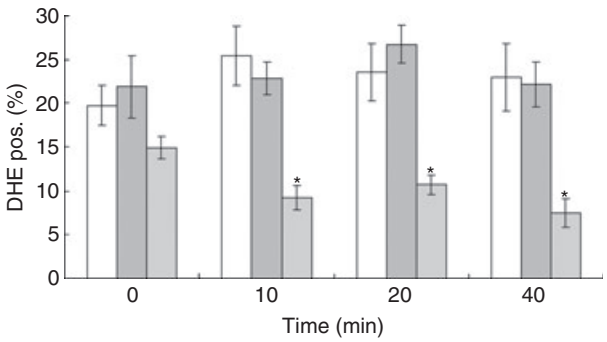

Figure 7 Levels of DHE accumulation after oxidative stress by H_2O_2. Cells in stationary state from the Δ*sip18* (white bars), *Δsip18, pGAL-GFP* (grey bars) and *Δsip18, pGAL-GFP-SIP18* strains (striped bars) were exposed to 4 mmol l^{-1} H_2O_2 and at the indicated times, aliquots were taken to evaluate DHE-positive (DHE pos.) cells. The represented data are the mean values ±SD from at least three independent experiments. *Indicates $P < 0{\cdot}01$ compared with both reference strains at each time.

Discussion

We have systematically screened a haploid, single gene deletion mutant library and identified 116 genes that are essential to desiccation tolerance. To our knowledge, this is the first systematic screen for the identification of putative genes essential to overcoming the cell dehydration process. The broad range of identified mutants indicates that these genes are involved directly or indirectly in dehydration tolerance. Attempts have recently been made

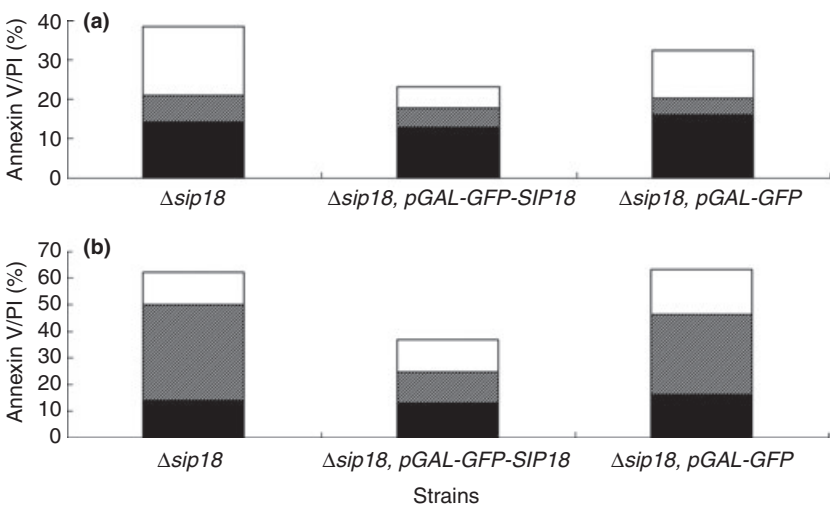

Figure 6 Overexpression of SIP18p prevents necrotic cell death. Quantification of stained cells: V^-/PI^+ □, V^+/PI^+ ▨ and V^+/PI^- ■; before drying (a) and after rehydration (b). The represented values are means of $n = 3$ determinations, and the SD was <10%. In each experiment, 5×10^6 cells were evaluated.

to describe the early transcriptional response of both wine yeasts and the BY4742 haploid strain during the process of drying and rehydration, and they have shown changes in the expression of genes involved in lipid binding and synthesis, protein synthesis and metabolism (Singh *et al.* 2005). The genes reported to show transcription activation early on in the rehydration or inoculation steps are consistent with the idea that some of them might be essential to the cell's ability to recover from desiccation stress. The hypersensitivity of the mutants to dehydration of the heat shock protein HSP30p, the 6-phosphofructokinase alpha subunit PFK1p, the epimerase peroxisomal FOX2p, the ribosomal protein RPS1Ap, the RNA polymerase A chain RPA49p and the uncharacterized osmotic stress protein SIP18p allows us to draw a parallel with the relatively early gene activation previously observed. Our results explain the fact that overexpressing *SIP18* impedes yeast mortality during the imposition of dehydration stress. The induction of *SIP18* transcription in response to osmotic stress suggests that this hydrophilin represents a broad adaptation to water deficit (Posas *et al.* 2000). Our observations showed a rapid nuclear accumulation of SIP18p in response to osmotic stress and cell dehydration stress. However, when osmotic stress was induced by adding 0·5 mol l^{-1} NaCl to the culture medium, such nuclear accumulation was not observed. As well was described found that the transcriptional regulation response to the addition of 0·5 mol l^{-1} NaCl is slightly different from that observed when 1 mol l^{-1} sorbitol is added, which corresponds to the same osmotic pressure for 0·5 mol l^{-1} NaCl (Hirasawa *et al.* 2006). However, the difference decreases under 0·75 mol l^{-1} NaCl and 1 mol l^{-1} sorbitol addition conditions when the dynamics of the changes in gene expression are similar. Yet the difference in SIP18p cytolocalization when adding sorbitol as opposed to NaCl was considerable, suggesting that this variation might not be driven by differential transcription regulation. The effects of osmotic pressure associated with sodium and chloride ion toxicity prevented the import of SIP18p into the nucleus. In this hypertonic condition (containing more than 0·8 mol l^{-1} NaCl), yeast cells show an increase in both the generation of superoxide species and the oxidation of cellular low molecular weight thiols and a decrease in the total antioxidant capacity of cellular extracts (Koziol *et al.* 2005). Another effect induced by exposure to this hypertonic medium is the modification of intracellular phosphotransfer rates, as was described within the SLN1-YPD1-SSK1 phosphorelay (Kaserer *et al.* 2009). If superoxide abolishes the export of SIP18p, one should expect antioxidant complementation to be able to scavenge superoxide. In that case, a correlation of SIP18p nuclear localization resulting from the reaction with superoxide and the antioxidant studied would be expected. However, the cells under ionic–hypertonic stress do not show any nuclear fluorescence in the presence of ascorbic acid. Although cells overexpressing SIP18p show twice as few true necrotic cells before stress imposition, Annexin V^-/PI^+ cells for all the strains do not exhibit a significant statistical increase after rehydration. We assume that dehydration stress is very aggressive for the cell and the accumulation of 'secondary necrotic' cells after stress imposition is made up of the physically and chemically damaged cells and the resulting cells from the apoptotic death process, which results in a loss in plasma membrane integrity (Eisenberg *et al.* 2010). The SIP18p-specific cytolocalization during stress imposition allows us to hypothesize that Sip18p may be involved in preventing cell death–regulating factors such as Apoptotic Inducer Factor 1, or the major mitochondrial nuclease NUC1 from passing from the cytosol to the nucleus, or by confining pronecrotic yeast, homologue to the mammalian high-mobility group box-1 protein, Nhp6Ap to the nuclear space (Carmona-Gutierrez *et al.* 2010).

Here, we have shown that SIP18p acts as an inhibitor of apoptosis in yeast under dehydration stress, suggested by its antioxidative capacity through the reduction of ROS accumulation after an H_2O_2 attack. *SIP18* was originally identified as a gene inducible by ionic osmotic stress (Miralles and Serrano 1995). Hydrophilin research in different organisms has allowed us to make significant advances towards understanding some of their biological properties, including their roles as antioxidants and as membrane and protein stabilizers during water stress, either by direct interaction or by acting as a molecular shield (Tunnacliffe and Wise 2007). Recent data provide evidence that SIP18p allows the cell to survive probably by acting to stabilize other cellular proteins, as described for XIAPp (Dohi *et al.* 2004) and BIR1p (Walter *et al.* 2006), rather than by directly interacting with apoptotic proteins in the nucleus, thereby inhibiting them. With recent advances in tissue engineering, cell transplantation and genetic technology, successful long-term storage of living cells is of critical importance. The complex regulatory network and the often contradictory results associated with high eukaryotic cells make the application of a simpler model system desirable. A number of advantages have made yeast cells the model of choice for anhydrobiotic engineering, including the ease of growth and modification, well-characterized cell physiology, genetics and biochemistry.

Acknowledgements

This work was supported by grant AGL2009-07933 from the Spanish *Ministerio de Ciencia e Innovación*.

References

Battaglia, M., Olvera-Carrillo, Y., Garciarrubio, A., Campos, F. and Covarrubias, A. (2008) The enigmatic LEA proteins and other hydrophilins. *Plant Physiol* **148**, 6–24.

Botstein, D., Chervitz, S.A. and Cherry, J.M. (1997) Yeast as a model organism. *Science* **277**, 1259–1260.

Brachmann, C.B., Davies, A., Cost, G.J., Caputo, E., Li, J., Hieter, P. and Boeke, J.D. (1998) Designer deletion strains derived from *Saccharomyces cerevisiae* S288C: a useful set of strains and plasmids for PCR-mediated gene disruption and other applications. *Yeast* **14**, 115–132.

Büttner, S., Eisenberg, T., Herker, E., Carmona-Gutierrez, D., Kroemer, G. and Madeo, F. (2006) Why yeast cells can undergo apoptosis: death in times of peace, love, and war. *J Cell Biol* **175**, 521–524.

Carmona-Gutierrez, D., Eisenberg, T., Büttner, S., Meisinger, C., Kroemer, G. and Madeo, F. (2010) Apoptosis in yeast: triggers, pathways, subroutines-Review. *Cell Death Differ* **17**, 763–773.

Coligan, J.E., Dunn, B.M., Speicher, D.W. and Wingfield, P.T. (2000) *Current Protocols in Protein Science*. Hoboken, NJ: John Wiley & Sons, Inc.

Crowe, J.H., Hoekstra, F.A. and Crowe, L.M. (1992) Anhydrobiosis. *Annu Rev Physiol* **54**, 579–599.

Dohi, T., Okada, K., Xia, F., Wilford, C.E., Samuel, T., Welsh, K., Marusawa, H., Zou, H. *et al.* (2004) An IAP-IAP complex inhibits apoptosis. *J Biol Chem* **279**, 34087–34090.

Eisenberg, T., Carmona-Gutierrez, D., Büttner, S., Tavernarakis, N. and Madeo, F. (2010) Necrosis in yeast. *Apoptosis* **15**, 257–268.

Gasch, A.P., Spellman, P.T., Kao, C.M., Carmel-Harel, O., Eisen, M.B., Storz, G., Botstein, D. and Brown, P.O. (2000) Genomic expression programs in the response of yeast cells to environmental changes. *Mol Biol Cell* **11**, 4241–4257.

Goyal, K., Walton, L.J. and Tunnacliffe, A. (2005) LEA proteins prevent protein aggregation due to water stress. *Biochem J* **388**, 151–157.

Hirasawa, T., Ashitani, K., Yoshikawa, K., Nagahisa, K., Furusawa, C., Katakura, Y., Shimizu, H. and Shioya, S. (2006) Comparison of transcriptional responses to osmotic stresses induced by NaCl and sorbitol additions in *Saccharomyces cerevisiae* using DNA microarray. *J Biosci Bioeng* **102**, 568–571.

Hjelmqvist, L., Tuson, M., Marfany, G., Herrero, E., Balcells, S. and Gonzàlez-Duarte, R. (2002) ORMDL proteins are a conserved new family of endoplasmic reticulum membrane proteins. *Genome Biol* **3**, research0027.1-0027.16.

Huh, W.-K., Falvo, J.V., Gerke, L.C., Carroll, A.S., Howson, R.W., Weissman, J.S. and O'Shea, E.K. (2003) Global analysis of protein localization in budding yeast. *Nature* **245**, 686–691.

Jansen, G., Wu, C., Schade, B., Thomas, D.Y. and Whiteway, M. (2005) Drag & drop cloning in yeast. *Gene* **344**, 43–51.

Kaserer, A.O., Andi, B., Cook, P.F. and West, A.H. (2009) Effects of osmolytes on the SLN1-YPD1-SSK1 phosphorelay system from *Saccharomyces cerevisiae*. *Biochemistry* **48**, 8044–8050.

Koziol, S., Zagulski, M., Bilinski, T. and Bartosz, G. (2005) Antioxidants protect the yeast *Saccharomyces cerevisiae* against hypertonic stress. *Free Radic Res* **39**, 365–371.

Madeo, F., Frohlich, E. and Frohlich, K.U. (1997) A yeast mutant showing diagnostic markers of early and late apoptosis. *J Cell Biol* **139**, 729–734.

Miralles, V.J. and Serrano, R. (1995) A genomic locus in *Saccharomyces cerevisiae* with four genes up-regulated by osmotic stress. *Mol Microbiol* **17**, 653–662.

Miyao, T., Barnett, J.D. and Woychik, N.A. (2001) Deletion of the RNA polymerase subunit RPB4 acts as a global, not stress-specific, shut-off switch for RNA polymerase II transcription at high temperatures. *J Biol Chem* **276**, 46408–46413.

Piper, P.W., Ortiz-Calderon, C., Holyoak, C., Coote, P. and Cole, M. (1997) Hsp30, the integral plasma membrane heat shock protein of *Saccharomyces cerevisiae*, is a stress-inducible regulator of plasma membrane H(+)-ATPase. *Cell Stress Chaperones* **2**, 12–24.

Posas, F., Chambers, J.R., Heyman, J.A., Hoeffler, J.P., de Nadal, E. and Ariño, J. (2000) The transcriptional response of yeast to saline stress. *J Biol Chem* **275**, 17249–17255.

Potts, M. (2001) Desiccation tolerance: a simple process? *Trends Microbiol* **9**, 553–559.

Reyes, J.L., Rodrigo, M.J., Colmenero-Flores, J.M., Gil, J.V., Garay-Arroyo, A., Campos, F., Salamini, F., Bartels, D. *et al.* (2005) Hydrophilins from distant organisms can protect enzymatic activities from water limitation effects in vitro. *Plant Cell Environ* **28**, 709–718.

Rodríguez-Manzaneque, M.T., Ros, J., Cabiscol, E., Sorribas, A. and Herrero, E. (1999) Grx5 Glutaredoxin plays a central role in protection against protein oxidative damage in *Saccharomyces cerevisiae*. *Mol Cell Biol* **19**, 8180–8190.

Rodríguez-Porrata, B., Novo, M., Guillamón, J., Rozès, N., Mas, A. and Cordero-Otero, R. (2008) Vitality enhancement of the rehydrated active dry wine yeast. *Int J Food Microbiol* **126**, 116–122.

Rodríguez-Porrata, B., Lopez, G., Redón, M., Sancho, M., Rozès, N., Mas, A. and Cordero-Otero, R. (2011) Effect of lipids on the desiccation tolerance of yeasts. *W J Microbiol Biotech* **27**, 75–83.

Sambrook, J. and Russell, D.W. (2001) *Molecular Cloning, a Laboratory Manual*. New York: Cold Spring Harbor Laboratory Press.

Singh, J., Kumar, D., Ramakrishnan, N., Singhal, V., Jervis, J., Garst, J.F., Slaughter, S.M., DeSantis, A.M. *et al.* (2005) Transcriptional response of *Saccharomyces cerevisiae* to desiccation and rehydration. *Appl Environ Microbiol* **71**, 8752–8763.

Smirnova, M., Van Komen, S., Sung, P. and Klein, H.K. (2004) Effects of tumor-associated mutations on Rad54 functions. *J Biol Chem* **279**, 24081–24088.

Teixeira, M.T., Arneric, M., Sperisen., P. and Lingner, J. (2004) Telomere length homeostasis is achieved via a switch between telomerase- extendible and -nonextendible states. *Cell* **117**, 323–335.

Tunnacliffe, A. and Wise, M.J. (2007) The continuing conundrum of the LEA proteins. *Naturwissenschaften* **94**, 791–812.

Walter, D., Wissing, S., Madeo, F. and Fahrenkrog, B. (2006) The inhibitor-of-apoptosis protein Bir1p protects against apoptosis in *S. cerevisiae* and is a substrate for the yeast homologue of Omi/HtrA2. *J Cell Sci* **119**, 1843–1851.

Zhang, L., Ohta, A., Takagi, M. and Imai, R. (2000) Expression of plant group 2 and group 3 *lea* genes in *Saccharomyces cerevisiae* revealed functional divergence among LEA proteins. *J Biochem (Tokyo)* **127**, 611–616.

Supporting Information

Additional Supporting Information may be found in the online version of this article:

Table S1 Primers designed for PCR.

Please note: Wiley-Blackwell are not responsible for the content or functionality of any supporting materials supplied by the authors. Any queries (other than missing material) should be directed to the corresponding author for the article.